Sensitivity analysis in the technical potential assessment of onshore wind and ground solar photovoltaic power resources at regional scale
-
Supplementary material

Arthur Bossavy[1], Robin Girard[2], and George Kariniotakis[3]

[1,2,3]MINES ParisTech, PSL - Research University,, PERSEE - Center for Processes, Renewable Energies & Energy Systems,, CS 10207 rue Claude Daunesse, 06904 Sophia Antipolis Cedex, France.

Corresponding author email: abossavy@gmail.com

1 Data and modeling for wind and solar power potential assessment

1.1 Data and modeling for wind power production simulation

1.1.1 Spatial interpolation of MERRA wind speed data using ECMWF reanalysis data

We used a statistical linear model to infer MERRA's wind speed $v_t^M(x^E)$, at time t and on some ECMWF grid point x^E included in the MERRA grid point x^M, from MERRA's estimate $v_t^M(x^M)$:

$$v_t^M(x^E) = a_t^{x^E} v_t^M(x^M) + b_t^{x^E},$$

where the coefficients $a_t^{x^E}$ and $b_t^{x^E}$ are estimated using ECMWF's wind speed estimate $v_t^E(x^E)$ as a response variable. This estimation is carried out adaptively on a monthly basis, from a sample whose size is defined by the ECMWF data temporal resolution (4 measurements per day x 30 days a month = 120 observations)

1.1.2 Statistical regional power curve model

Denoting by p_t the regional wind power production and by $\overline{v_t}$ the weighted average wind speed, the piecewise statistical model can be written as:

$$p_t = a_1 \overline{v_t} \mathbb{1}_{\overline{v_t} \in [0,3]} + \mathcal{S}(\overline{v_t}) \mathbb{1}_{\overline{v_t} \in [3,10.5]} + a_2 \mathbb{1}_{\overline{v_t} \in [10.5,20]} + (a_3 \overline{v_t} + a_4) \mathbb{1}_{\overline{v_t} \in [20,24]},$$

where $a_1, a_2, a_4 > 0$, $a_3 < 0$ and $\mathcal{S}$ is a smoothing spline model [2] whose fitting is carried out to ensure continuity. Knots separating the various pieces of the model were estimated a priori based on trial and error. Figure 1 shows the resulting fit obtained for the French region of Brittany.

1.2 Data and modeling for solar power production simulation

1.2.1 Global horizontal irradiance data and projection on a tilted plan

In the Muneer projection model [3], we assumed that:

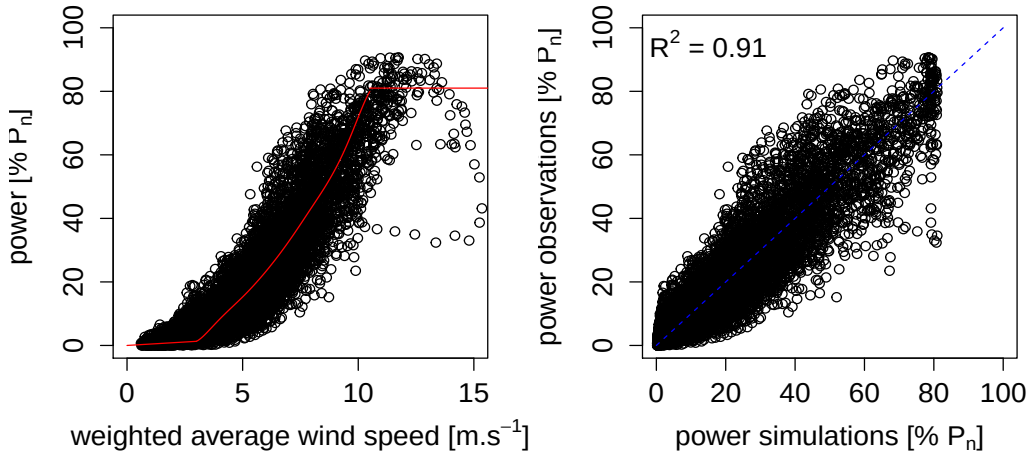

Figure 1: **Statistical regional power curve fit example** – Left: The fit giving the estimated power curve based on one year (2013) of hourly production data from the Brittany region. Right: Correspondance between observations and fitted values.

- Ground albedo used in the estimation of the ground reflected irradiance component is fixed at 0.2,
- The radiation distribution index used in the estimation of the isotropic part of the diffuse component is taken from [1].

1.2.2 Power conversion modeling

The following model was provided by our industrial partner Solais[1]. The electrical power P (in W) from PV modules depending on the irradiance level I (in W/m^2) reaching panels, is given by:

$$P = P_n \times \eta_{\text{mod}}(I) \times e^{\beta(T_c - T_{c_{\text{ref}}})} \times I, \tag{1}$$

where P_n is the installed capacity (in kWc), η_{mod} is the modules' efficiency depending on the irradiance level and relative to standard operating conditions (i.e. for $I = 1000$ W/m^2 and a reference cells' temperature $T_{c_{\text{ref}}} = 25°$C). In our study, η_{mod} was derived from a performance assessment of numerous products available on the market (taking the median performance profile, see Figure 2, left graph). The exponential factor in Equation (1) represents the thermal modeling of modules' efficiency depending on cells' temperature T_c. β is a thermal coefficient whose value depends on cells' technology ($\beta = -0.0043$ for mono- and polycristallin, $\beta = -0.002$ for thin film and $\beta = -0.0016$ for CPV).

In the considered model, cells' temperature is derived from the irradiance level and the ambient temperature T (provided by MERRA reanalysis), according to the following formula:

$$T_c = T + \frac{0.9}{U_c} \times (1 - R\eta_{\text{mod}}(I)) \times I,$$

where U_c is a thermal transfer coefficient, which depends on the installation set-up (since we are considering ground PV installations, we can assume that air circulation cooling devices are used, resulting in a high thermal transfer. Here, it has been set to $U_c = 29$) and R depends on the considered cells'

[1] http://www.solais.fr

technology ($R = 0.153$ for monocristallin, $R = 0.144$ for polycristallin, $R = 0.096$ for thin film and $R = 0.325$ for CPV).

Numerous losses at plant level, before and after the inverters, are taken into account through multiplicative coefficients. The final power delivered by the plant is thus:

$$P = \eta_{\mathrm{AC}} \times \eta_{\mathrm{inv}}(\eta_{\mathrm{DC}} \times P) \times \eta_{\mathrm{DC}} \times P,$$

where η_{DC} represents mismatch, spectral and other DC losses, while η_{AC} represents transformer, auxiliary, outage and other AC losses. The former was set at $\eta_{\mathrm{DC}} = 0.973$ for mono- and polycristallin, $\eta_{\mathrm{DC}} = 0.959$ for thin film and $\eta_{\mathrm{DC}} = 0.915$ for CPV. The latter was set at $\eta_{\mathrm{AC}} = 0.970$ and $\eta_{\mathrm{AC}} = 0.947$ for PV and CPV respectively. Similar to modules' efficiency depending on irradiance, the inverters' efficiency depending on load factor was derived from market products' performance assessment. The resulting median performance profile is shown in Figure 2 (right graph) for 4 different categories of inverter capacity. In our study, we consider large installations with an inverter capacity above 600 kVA.

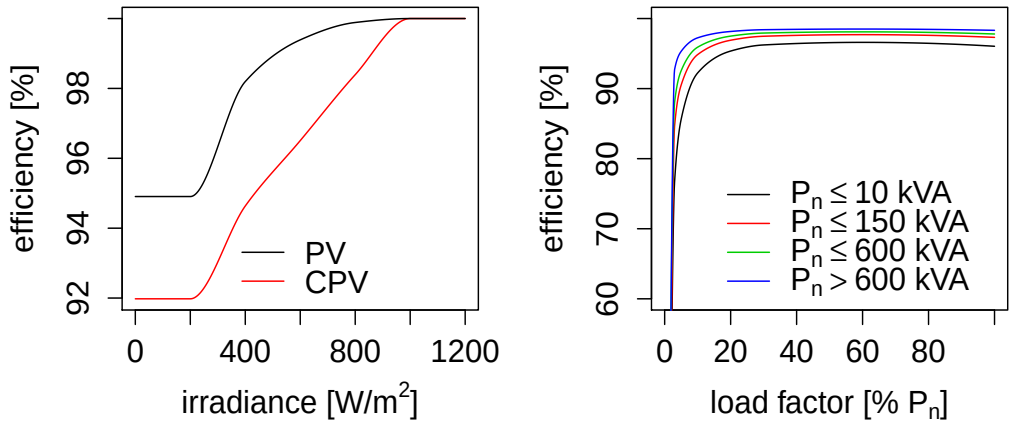

Figure 2: **PV modules and inverter efficiency (in %)**– Left: Modules' efficiency depending on the irradiance level for standard operating conditions. Right: Inverters' efficiency depending on load factor. In our study, the inverter capacity (P_n in this figure) was set at 0.9 times the module capacity.

1.2.3 CPV tracking systems

In our study, we consider both single- and dual-axis tracking systems associated with CPV technology. In the dual-axis tracking system, the panels' azimuth (i.e. orientation) angle is the same as the Sun's azimuth angle, while the panels' tilt (i.e. inclination) equals the Sun's zenithal angle. We integrated the technical limitations found in the description of the market products[2]. Thus, we imposed a panel tilt of $\alpha \leq 85°$ and a panel azimuth of $50° \leq \beta \leq 310°$. On the other hand, the considered singles-axis tracking system relies on a north-south horizontal axis with east-west panel inclination. This inclination can never exceed 50° and follows a backtracking algorithm[3] to maximize irradiance capture.

[2] Reference Exosun, see http://www.exosun.fr

[3] Provided by Solais. In this algorithm, at sunrise and sunset, a more horizontal inclination of panels is preferable because the isotropic diffuse irradiance level is higher than the direct irradiance level.

1.3 Geographical constraints and potential assessment methodology

1.3.1 Corine Land Cover 2006 database and acceptability ratios

Table 1 describes the Corine Land Cover 2006 database and associated acceptability ratio values r_{lc} (see the paper, Section 2.3.2, for a description of the role of such a ratio). While only one ratio value is considered for PV (to keep the number of parameters reasonable in the sensitivity analysis), 4 different values are considered for wind power (denoted by WP in Table 1): r_{lc_a}, r_{lc_f}, r_{lc_w} and $r_{lc_{dv}}$. Subscripts a, f and w denote categories of surfaces on which turbines are to be installed: agricultural, forest and wet surfaces. The subscript dv is associated with surface types subject to special attention. Indeed, higher acceptability ratio values might be envisaged on such surfaces, as assumed in [4].

Table 1: Corine Land Cover 2006 database and associated acceptability ratio values r_{lc}.

Code	Description	WP ratio	PV ratio
111	continuous urban area	0	0
112	discontinuous urban area	0	0
121	industrial and commercial area	0	0
122	road and train network	0	0
123	port	0	0
124	airport	0	0
131	material extraction	0	0
132	garbage dump	0	0
133	construction site	0	0
134	urban green area	0	0
135	sport and leisure dedicated area	0	0
211	non-irrigated arable land	r_{lc_a}	0
212	irrigated land	r_{lc_a}	0
213	rice field	r_{lc_a}	0
221	vineyard	r_{lc_a}	0
222	orchard	r_{lc_a}	0
223	olive grove	r_{lc_a}	0
231	meadow	$r_{lc_{dv}}$	0
241	annual farming	r_{lc_a}	0
242	fragmented cultural area	r_{lc_a}	0
243	natural, sparsely farmed area	r_{lc_a}	r_{lc}
244	forest-agricultural land	r_{lc_a}	0
311	lobed-leaved tree forest	r_{lc_f}	0
312	conifer forest	r_{lc_f}	0
313	mixed tree forest	r_{lc_f}	0
321	grass and pastureland	$r_{lc_{dv}}$	r_{lc}
322	moors and bushes	$r_{lc_{dv}}$	r_{lc}
323	sclerophyll plants	r_{lc_f}	r_{lc}
324	shrubby plants	r_{lc_f}	0
331	sand, beach, dune	0	0
332	rock	0	0
333	sparse vegetation	$r_{lc_{dv}}$	r_{lc}
334	burned area	$r_{lc_{dv}}$	r_{lc}
335	glacier, permanent snow	0	0
411	marsh	r_{lc_w}	0
412	peatland	r_{lc_w}	0
421	maritime marsh	0	0
422	salt marsh	r_{lc_w}	0

Code	Description	WP ratio	PV ratio
423	coastline area	0	0
511	river	0	0
512	pool, pond, lake	0	0
521	lagoon	0	0
522	estuary	0	0
523	sea, ocean	0	0

1.3.2 Installed capacity per surface unit at power plant scale

In this paper, we differentiate the value of coefficient c_u associated with standard wind turbine technology or PV installations with fixed orientation (in Section 4.2, Table 1), and the value by which all technologies from the technology mix are being considered (in Section 2.3.2).

For wind power, the final parameter value is estimated from that associated with standard turbine technology c_u, assuming that new technology's installed capacity per surface unit is equal to $\frac{2}{3}c_u$ (as in [4]), and using a weighted average based on installed capacity proportions:

$$c_u = (1 + (2/3 - 1)w_{\mathrm{wp}_n})c_u,$$

where w_{wp_n} is the proportion of installed capacity with new wind turbine technology.

We use the same procedure for ground PV. We assume that installations with single-axis tracking systems have the same installed capacity per surface unit c_u as installations with fixed orientation. Assuming that for installations with dual-axis tracking system such a parameter equals $\frac{c_u}{2}$ (still as in [4]). Then, the final value of c_u is given by:

$$c_u = (1 - 0.5w_{t_2})c_u,$$

where w_{t_2} is the installed capacity proportion of installations with a dual-axis tracking system.

2 Methodology for the sensitivity analysis

2.1 Observation binning procedure in the Sobol indices computation

Observation bins result from rounding off input values. The objective is to "keep a balance" between excessive rounding of input values and defining sufficiently populated bins. However, this process does not rely on any objective criteria. Coarser rounding was used when computing higher order Sobol indices (i.e. using multi-dimensional bins). Rounding information for the various parameters is summarized in Table 2.

Table 2: Rounding of parameter values to create observation bins. Rounding accuracy varies depending on which Sobol index order is to be computed. The usual ratios are expressed in percentages here. WP denotes wind power, PV photovoltaic power and P_n the power plant's nominal capacity.

Parameters	1st order	higher order
h_{wp_n}, w_{wp_n}, h_{pv}, w_p, w_a, w_{t_1}, w_{t_2}	1%	for WP: 5%, for PV: 10%
$c_{\min}$, r_{lc_a}, r_{lc_f}, r_{lc_w}, $r_{lc_{dv}}$, r_{lc}	0.1%(P_n)	1%(P_n)
c_u	for WP: 0.1W, for PV: 1W	1W
α, β, β^{north}	2°	2° (for β^{north}: 10°)
$\mathrm{alt}_{\max}$	100m	100m
$\nabla\mathrm{alt}_{\max}$, $\nabla\mathrm{alt}_{\max}^{\mathrm{north}}$	2%	10%

References

[1] E. G. Evseev and A. I. Kudish. The assessment of different models to predict the global solar radiation on a surface tilted to the south. *Solar Energy*, 83(3):377 – 388, 2009.

[2] T. Hastie, R. Tibshirani, and J. Friedman. *The elements of statistical learning, second edition: Data mining, inference, and prediction.* Springer Series in Statistics. Springer, 2nd ed. 2009. corr. 3rd printing edition, 2009.

[3] T. Muneer. *Solar radiation and daylight models for the energy efficient design of buildings.* Architectural Press, 1997.

[4] Agence Departementale pour l'Environnement et la Matrise de l'Energie. Cap 100% EnR 2050: Simulation de la production renouvelable et valuation des gisements. Technical report, 2015.